Estimate of fine sediment deposit dynamics over a gravel bar using photography analysis

B. Camenen, M. Jodeau, M. Jaballah

Author-produced version of the article published in International Journal of Sediment Research (2013), Vol. 28, Iss. 2, 220–233
The original publication is available at http://www.sciencedirect.com/ doi:10.1016/S1001-6279(13)60033-5

Estimate of fine sediment deposit dynamics on a gravel bar using photography analysis

B. CAMENEN[1], M. JODEAU[2], and M. JABALLAH[3]

Abstract

Three different methods to analyse fine sediment deposits on a gravel bar using pictures are presented in this paper. A manual digitization and deposits zone delineation are performed as well as two different automated procedures. The three methods are applied on aerial pictures taken in 2006 by a drone from a height around 150 m above the study site. Two other sets of pictures taken in 2010 are also studied: the first set was obtained from the left side bank of the river at approximately 15m above the gravel bar whereas the second one was taken from a helicopter flying 600 m above the ground. These methods were used to estimate the surface of fine sediment deposits before and after flushing events. They yield similar results even if the first automated procedure is able to capture smaller patches of fine sediments. The total surface of fine sediment deposits seems to be similar before and after a flushing event, but the distribution appears quite different. Before a flushing event, a significant amount of fine sediment deposits are mixed with coarser sediments. After the flushing event, one can observe more large fine sediment deposits located on the downstream part of the secondary channel and at the channel margin. Most of the small fine sediment deposit patches were washed out. A short discussion is provided on the possible dynamics of fine sediment deposits over the gravel bar.

Key words: fine sediment deposits, photo analysis, automated procedure, flushing event

1 Introduction

Many of the Alpine river systems are regulated by hydro-power reservoirs. These mountain streams are not only affected by the continuous effects of dams on sediment transport but they are also occasionally impacted by reservoir releases. Liu et al. (2004) stated that the annual worldwide loss rate of reservoirs storage capacity due to sedimentation is 0.5 % - 1.9 %. The flushing of fine sediments from reservoirs into downstream channels is an ordinary practice, as it is an essential operation to ensure stream dams efficiency (Morris and Fan, 1996). However, reservoir releases may often have significant effects on downstream river reaches due to the high flows induced by the sudden release of water and high concentration of fine sediments (Ma et al., 2012). A high concentration of suspended sediments may impact the downstream aquatic environment by modifying fish survival conditions or limiting their habitat due to clogging of interstices (Liu et al., 2004). When the transport capacity of the downstream channel is sufficiently reduced, the finer sediment may accumulate on the bed of the river (Kondolf and Wilcock, 1996). Wohl and Cenderelli (2000) and Rathburn and Wohl (2003) showed that fine sediment deposition occurs primarily in pools and in lateral eddies. Flow duration and velocity magnitude govern the volume and grain size distribution. Brandt (1999) established that fine sediments mainly deposit on the channel bed instead of riverbanks in downstream reaches of a flushed reservoir. Such deposits impact the sedimentary construction of the river and may also lead to stratifications (Wang et al., 2008). Changes in channel morphology and large deposits of fine sediments may also have an impact on the vegetation dynamics in the river channel and on fish habitat as observed by Lisle (1989) and Wood and Armitage (1997).

The downstream reaches of mountain streams are generally either braided or, in the case of embanked streams, alternate bar channels. In rivers with high fine sediment yield, fine sediment deposits may have a strong impact on gravel bar stability especially due to their interaction with vegetation. The development of gravel bars and pools is essential for spawning habitat for fish, and for rheophilic invertebrate species but their habitat conditions remain very sensitive to grain size distribution (Rubin et al., 2004). In a flooded regulated river, Grams and Schmidt (2004) showed that the aggradation of the downstream reach was accompanied with fine sediments accumulation along riverbanks and gravel bars in the absence of high intensity flows. Gravel bars have a significant

[1] Dr, Research scientist, *Irstea, HHLY, 3 bis quai Chauveau, CP 220, 69336 Lyon cedex 09, France*
[2] Dr, Research scientist, *EDF-LNHE, 6 quai Watier, 78401 Chatou cedex, France*
[3] PhD candidate, *Irstea, HHLY, 3 bis quai Chauveau, CP 220, 69336 Lyon cedex 09, France*

Author-produced version of the article published in International Journal of Sediment Research (2013), Vol. 28, Iss. 2, 220–233
The original publication is available at http://www.sciencedirect.com/ doi:10.1016/S1001-6279(13)60033-5

importance in grain sorting and sediment transfer along the river (Folk and Ward, 1957; Konrad, 2002). Thus, it requires analysis of the surface grain size of rivers as a continuously varying patchy environment (Fausch et al., 2002).

In the recent years, several authors suggested various methodologies to estimate surface grain size distribution based on aerial photographies (Lyon et al., 1992; Carbonneau et al., 2005a, 2005b; Verdúa et al., 2005). Grain size is often empirically related to texture or semivariance value (Carbonneau et al., 2004). Such a methodology was validated for coarse sediments with grain size larger than a few centimetres but it still needs to be improved for finer sediments.

The purpose of this paper is to better describe fine sediment deposits over a gravel bar and to understand their dynamics. This study deals with field measurements of deposit repartition over a gravel bar before and after dam flushes using photography analysis. The field study is located in the downstream part of the Arc River (France), where flushing of the three upstream river dams is carried out every year in late spring. For two different events (in 27th June 2006 and in 8th June 2010), three different methodologies were applied on the same gravel bar and compared. In 2010, aerial pictures taken from LiDAR survey (one month before and three months after the flushing event) were also analysed in order to discuss the proposed methodology and results.

2 Description of study area and methodologies used to study fine sediment deposits

2.1 Description of study area

The fieldwork takes place in the Arc River which rises in the French Alps (Fig. 1). The Arc River watershed area is 1957 km^2. The hydrological regime is nival with natural discharges higher during snow melt. The ten year return period flood is approximately 300 m^3/s and the mean winter discharge is 6-8 m^3/s. The river bed has been recalibrated in order to allow the 1 km wide valley to contain a road, a highway and a railway. Consequently, the river has been artificially straightened in many places. Only 5% of the river reaches remain with their natural flow patterns and morphology. In addition the flow is regulated by many hydraulic constructions (several dams and pipes) for hydroelectricity production. The present regulated flow regime has significantly altered the natural river discharges and sediment transport. Although its bed is made of gravel, the River Arc has unusually high fine sediment transport, supplied by tributaries. The main ones are the Arvan and Glandon streams which supply large amounts of predominantly black lias schist. The area of interest is restrained to one single alternate gravel bar located on the left side of the river, 200 m upstream from a bridge, 18 km downstream Saint-Martin-la-Porte reservoir (see Fig. 1). Lateral limits are set by 5 m high embankments made of boulders and scattered young trees. The mean slope of this reach is approximately 0.6 %.

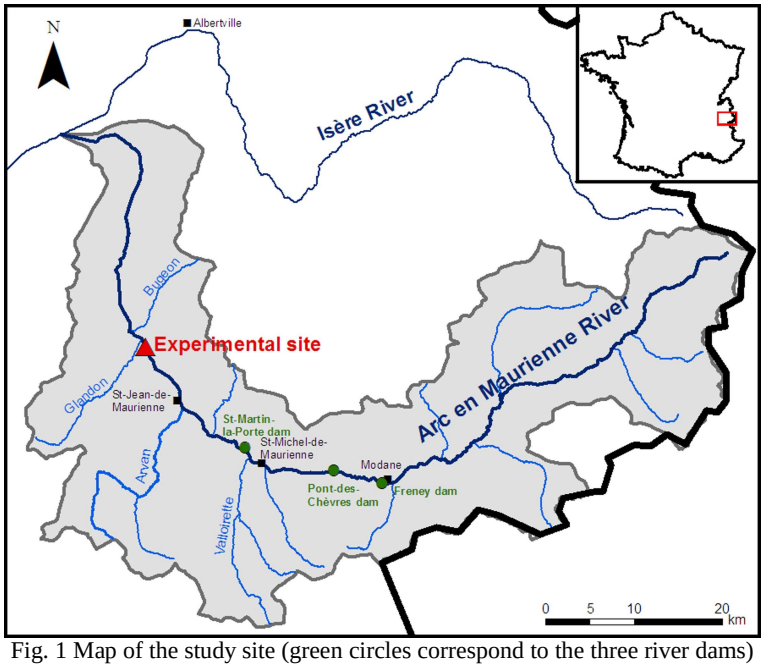

Fig. 1 Map of the study site (green circles correspond to the three river dams)

On the gravel bar, the grain size distribution is poorly sorted and typical median grain size

Author-produced version of the article published in International Journal of Sediment Research (2013), Vol. 28, Iss. 2, 220–233
The original publication is available at http://www.sciencedirect.com/ doi:10.1016/S1001-6279(13)60033-5

diameter varies from 10 cm (bar head) to 2 cm (bar tail). Fine sediment deposits that are observed on the gravel bar are composed of a sand and silt mixture (grain size varying from 30 to 400 μm). A detailed description of this specific gravel bar and its morphological units has been given in Jodeau (2007b).

Most of the fine sediment flux occurs during snow melt season (May to July), but sediments are trapped in the reservoirs throughout the year and flushed downstream when the reservoirs are drained. The three reservoirs located in the middle part of the River Arc are flushed once a year. Otherwise they would rapidly fill with fine sediments and could not be able to regulate discharge for hydro-power production. The mass of flushed sediments during the previous releases was roughly estimated by hydro-power plants managers to be between 20×10^3 and 150×10^3 tons. Flushing flows are completed as counterpart to mechanical dam cleaning. The flushing operation is performed as follows: (i) the flow is first released from the flap gates that produce clear water (10 m^3/s); then (ii) deep gates are opened, the discharge is increased gradually to reach the maximum discharge in 6 hours; (iii) the peak discharge is maintained for 2 hours; and finally, (iv) the water discharge is decreased gradually. For the studied release, dam managers estimated the maximum peak discharge to be 130 m^3/s approximately, which is equivalent to a one year return period flood. The maximum sediment concentration varies from 10 to 30 g/l. For both surveys, the flushing event was the only event for which the gravel bar was submerged. In 2010, a natural flood with a 200 m^3/s peak discharge occurred on 16th - 17th June; no significant event occurred thereafter until the following LiDAR survey.

2.2 Methodologies used to estimate the surface of fine sediment deposits

The methodologies proposed here are based on georeferenced, orthorectified and high-quality (1 pixel ≤ 5cm) photographs of the gravel bar (using at least six artificial, regularly distributed, ground reference points per picture) to identify preferential places of fine sediment deposits. Based on the fact that gravel areas appear on photographs whiter and less uniform than fine sediment patches, the latters were identified on the bar as zones with clearly uniform grey colour. As a first attempt, patch contours were eventually manually digitized (procedure 1). Automated procedures, which are capable of quantifying the extent of fine deposit patches in image were also developed (procedures 2 and 3).

For the first event (2006), aerial photographs of the reach were taken from a drone (19 days before and 8 days after the event), which was flying 150 m above the ground approximately. The used camera was a Canon Powershot G5 5Mpixels or a G3 4Mpixels leading to a resolution of 5 cm per pixel on the ground on average. Aerial photographs have the advantage to be nearly vertical but the drone was not stable and dangerous to drive; therefore, it was not used again.. For the second event (2010), photographs were taken from a high-lift truck set on the side bank of the river at 15 m above the gravel bar approximately (4 days before and 1 day after the event) using a Pentax OptioW60 10Mpixels camera. The angle of exposure being relatively low, a significant deformation of the images is observed after ortho-rectification. For this campaign, one pixel represents 4 cm on the ground on average, corresponding to the original resolution in the zone of interest. A third additional set of images was used, two LiDAR surveys were performed in 9th May and 5th September 2010. Images were taken from a helicopter flying 600 m above the ground using a Hasselblad camera with a 50 mm objective. The image definition is of 0.08 m.

2.2.1 Procedure 1: manual methodology

Procedure 1 is a non automatic method to recognize the fine sediment deposit. The user identifies the boundaries of fine sediment patches. Patch contours were eventually manually digitized using ArcMap tools. Manual delineation is user dependent, and can be time consuming. But it doesn't require any programming. This procedure was applied for the 2006 flushing event.

2.2.2 Procedure 2: spectral and textural analysis (Envi4.3 methodology)

In 2006, the analysis was achieved using commercial softwares (Jodeau, 2007a). Images were rectified and georeferenced using ArcMap. Envi4.3 software was then used (i) to extract the area of interest (gravel bar) (ii) to adjust colours from a reference image and (iii) to gather all images into a mosaic. Identification of fine sediment deposits on the images was performed following two main steps:

The first step consists of a spectral analysis. For each class defined (vegetation, white gravels, clear fine deposits, dark fine deposits, and marker), a region of interest (ROI) is defined on the picture from the Red Green Blue (RGB) values of each pixel. It plays the role of a reference value for the class. The attribution of a class for each pixel is then completed using the minimum distance classification. The result is exported in a raster with an integer for each class (Fig. 2(b)).

Author-produced version of the article published in International Journal of Sediment Research (2013), Vol. 28, Iss. 2, 220–233
The original publication is available at http://www.sciencedirect.com/ doi:10.1016/S1001-6279(13)60033-5

The second step consists of a textural analysis. Texture is an indicator of spatial patterns and their variability. Based on the work by Carbonneau et al. (2005a), image texture is evaluated with the co-occurrence matrix. The co-occurrence matrix is constructed by comparing all image pixels separated by a distance D at direction V. The element (i,j) of the co-occurrence matrix P for an image is the number of times that grey levels i and j occur in two pixels separated by distance D and direction V divided by the total number of pixel pairs. Therefore, the co-occurrence matrix P can quantify how many pixels of similar grey levels are neighbours. A windowing approach is used to produce a textural image, which retains local image texture properties using contrast (C) calculation:

$$C = \sum_{ij} (i-j)^2 P(i,j) \quad (1)$$

where i and j are the pixel position in the window.

The result is simplified using a threshold; pixels are then classified into two categories, homogeneous or not. The result is then exported in a raster format (Fig. 2(c)).

The third step consists in using an algebraic operation on the two rasters resulting from the two previous steps (Fig. 2(d)). To reduce noise, a smoothing method is applied by comparing the value of each pixel with its closest neighbours.

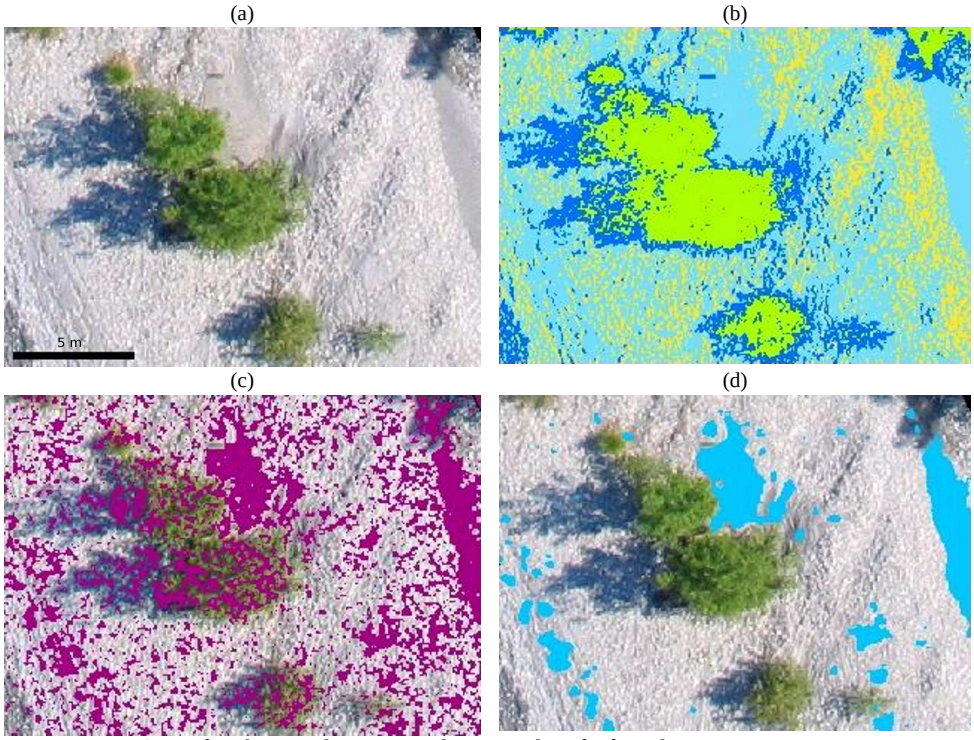

Fig. 2 Steps for the aerial image analysis to identify fine deposits repartition using Envi4.3: (a) original orthorectified image, (b) spectral analysis (green: vegetation, yellow: white gravels, light blue: clear fine deposits, dark blue: dark fine deposits) (c) textural analysis, and (d) final results.

2.2.3 Procedure 3: histogram characterisation

In 2010, a similar analysis was achieved using Matlab environment (procedure 3). Images were ortho-rectified using plan to plan transformation routines (Hauet, 2006). Images were converted into greyscale. The analysis of the images was then accomplished working on the histogram of sub-images using a similar windowing approach as presented above. Classes were defined for typical objects encountered in the pictures: trees, coarse white gravels, fine deposits, and mixture of fine and coarse sediments using the histogram of a $l_f \times l_f$ window (Fig. 3), with $l_f = 40$ pxl (1.6 m). Histograms for trees are dark and relatively wide; histograms for coarse gravels are white and relatively narrow; histograms for fine deposits are very narrow whereas histograms for fine and coarse sediment mixture are wide.

Author-produced version of the article published in International Journal of Sediment Research (2013), Vol. 28, Iss. 2, 220–233
The original publication is available at http://www.sciencedirect.com/ doi:10.1016/S1001-6279(13)60033-5

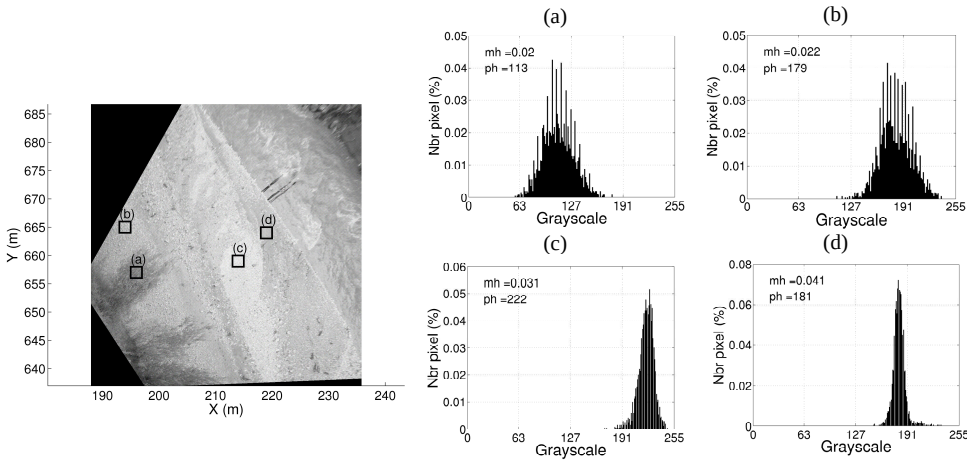

Fig. 3 Examples of histogram for different objects in the ortho-rectified photograph: (a) trees, (b) mixture fine and coarse sediments (c) coarse sediments, and (d) fine deposits.

In order to define precisely each of these classes, two parameters were calculated from the histogram: the pick value *ph* of the histogram, which gives an indication of the greyscale value, the mean value *mh* of the histogram filtered by values such as the number of pixels is higher than 1%, which gives an indication of the texture (the larger is *mh*, the narrower is the pick, and so the more uniform is the colour). Five classes were eventually distinguished. Their characteristics (conditions on *mh* and *ph*) are presented in Table 1. Water in the Arc River being dark with some white patterns due to foam, therefore, it was very difficult to assign a specific class for it. Images were then processed on the gravel bar only, excluding zones corresponding to the main channel using a geometric filter.

Table 1 Characteristics of the five classes of objects

No.	Description	Conditions on *mh*	Conditions on *ph*
(a)	Trees	$mh \leq 0.035$ if $90 < ph \leq 115$	$ph \leq 115$
(b1)	Mixture of fine and coarse sediments	$mh \leq 0.035$	$115 < ph \leq 165$
(b2)	Mixture of coarse and fine sediments	$mh \leq 0.035$	$165 < ph \leq 205$
(c)	Coarse sediments	-	$ph > 205$
(d)	Fine deposits	$mh > 0.035$	$90 < ph \leq 205$

A typical final result is presented is in Fig. 4. The used mesh for the windowing approach was set to $\Delta x = 10$ pxl (0.4 m) in both directions. Main classes appear to be clearly distinguished and vegetation properly discarded. It shows however that the size of the deposits are generally underestimated. This can be easily explained as the suggested thresholds for the five classes were defined for a homogeneous window with a size much larger than larger particles observed on the images (typically 1 to 2 pixels for our case). If $l_f = 40$ pxl, the histogram is more accurate (based on 1,600 values) but the risk to encounter non homogeneous window is higher. If $l_f = 10$ pxl, the histogram is not as accurate (based on 100 values) but the risk to encounter non homogeneous window is lower. It has been verified that the use of a smaller window size ($l_f = 10$ pxl) does not affect the threshold values obtained for a homogeneous window.

2.3 Comparison of the results obtained from procedures 2 and 3

In order to compare both automated methods, the image from 8th June 2006 presented in Fig. 2(a) was processed using the third method based on histograms. To show the impact of the window and mesh sizes, a smaller window was tested ($l_f = 10$ pxl or 0.4 m) as well as a finer mesh used for the windowing approach ($\Delta x = 2$ pxl or 0.08 m).

Results are presented in Fig. 5 and are coherent with results from the second method (Fig. 2(a)). However, procedure 3 appears more sensitive to the shadows (assimilated as trees or as a mixture of fine and coarse sediments). The second method based on colour spectrum can more easily treat vegetation thanks to the green colour. Because of the required size of the window needed to include a minimum of pixels to obtain a coherent histogram, procedure 3 cannot retrieve very small patches of fine deposits, which are assimilated to the fine and coarse sediment mixture. Similarly to the manual digitization achieved for the 2006 event (procedure 1, see Fig. 6a), only large patches are captured.

Author-produced version of the article published in International Journal of Sediment Research (2013), Vol. 28, Iss. 2, 220–233
The original publication is available at http://www.sciencedirect.com/ doi:10.1016/S1001-6279(13)60033-5

When a large window size is used, surface of deposits may be significantly underestimated (Fig. 5(a) with l_f = 40 pxl) as observed previously. On the other hand, the mesh density has limited impact on final results (Fig. 5(b) and (c)). Indeed, if the description of the deposit extent is more accurate using Δx = 2 pxl, the final computed surface is very similar. An underestimation by 20% of the surface is observed using Δx = 10 pxl; but it corresponds to the deposit located on of the image limits.

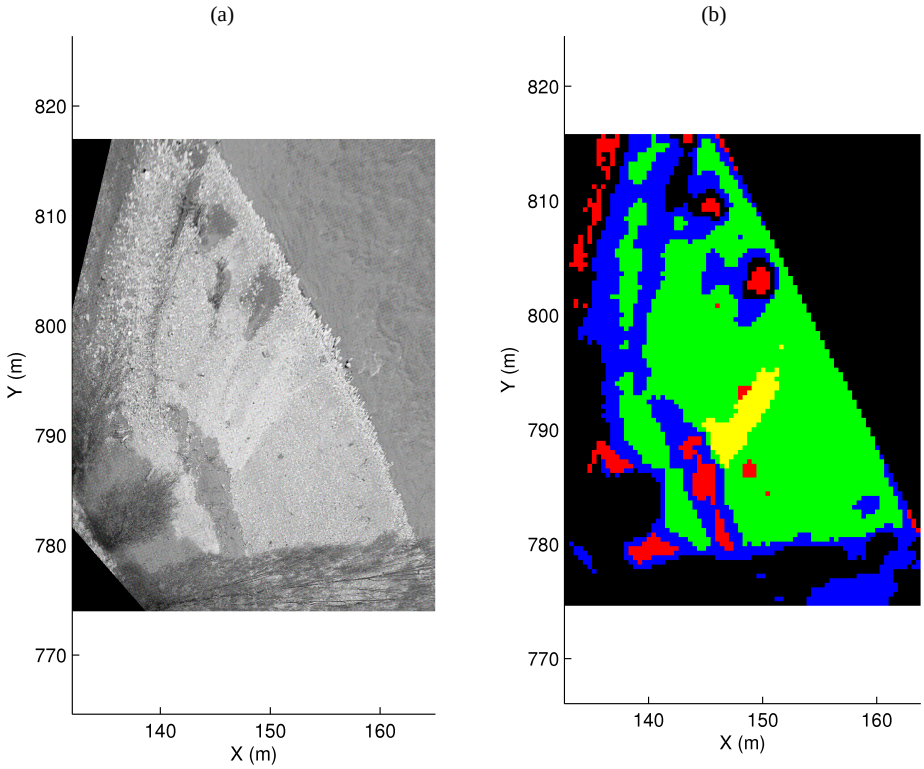

Fig. 4 Typical results from the automatic treatment of a greyscale picture into the five different classes (yellow: coarse sediments (c),green: mixture of fine and coarse sediments (b1), blue: mixture of coarse and fine sediments (b2), red: fine deposits (d), and black: trees) + geometric filter (a).

What is defined as a mixture of fine and coarse sediments (blue colour in procedure 3) often corresponds to deposits (as estimated using procedure 2) or to spurious results due to the presence of vegetation or shadow. For the latter case, it represents a limitation of the method if a too large window is used. What is defined as a mixture of coarse and fine sediments (green colour in procedure 3) also includes sometimes deposits as estimated in procedure 2. Based on field observation and on a close observation of pictures, a rough estimation of the percentage of fines deposits in the two classes of mixture would be: from 10 to 40% for the mixture of coarse and fine sediments (green colour) and 40 to 60% for mixture of fine and coarse sediments (blue colour). As an average, we will use hereafter 25% and 50%, respectively.

The influence of the light may also have some impact on the automatic treatment. From Fig. 5(c) to Fig. 5(d), only the delimitation between fines deposits and coarse sediments was changed (from 205 to 195). It yields a large increase of the estimated surface for the coarse sediment class. Similar difficulties were observed using procedure 2.

3 Results and discussion

3.1 Results for the 2006 flushing event using procedures 1, 2, and 3

It is interesting to see in Fig. 6 the differences between the results obtained by patch contours manually digitized using ArcMap tools (procedure 1) or using the methodology described in section 2.2.1 (procedure 2). If both methods indicate that fine sediment deposits are mainly located in the downstream part of the secondary channel and on the edge of the gravel bar (main channel margin), the expanse and exact position of the deposits differ significantly. The manual digitization tends to

Author-produced version of the article published in International Journal of Sediment Research (2013), Vol. 28, Iss. 2, 220–233
The original publication is available at http://www.sciencedirect.com/ doi:10.1016/S1001-6279(13)60033-5

limit the expanse of deposits to clear and relatively large deposits whereas the automated method estimates a larger expanse of deposits by including any small patch that could be considered as a sediments mixture together with surrounding coarse sediments. Using the manual digitization, one can quickly estimate the surface covered by fine sediment varying from 810 m^2 before the flushing event to 1,590 m^2 after the flushing event. Based on the automated method, the surface covered by fine sediment deposits on the bar appears to be nearly the same between both surveys before and after the 2006 event (Fig. 6(b))., i.e. 2,360 m^2 and 2,340 m^2, respectively. The differences may be explained as many of the deposits before the flushing correspond to small deposits scattered everywhere over the gravel bar (see blue colour in Fig. 6b). These deposits were not captured by the manual digitization. After the flushing event, these small deposits were replaced by large deposits located in the secondary channel and at the downstream part of the gravel bar. Thus, if the surface corresponding to large deposits increased after the flushing event, the total surface including small deposits is stable.

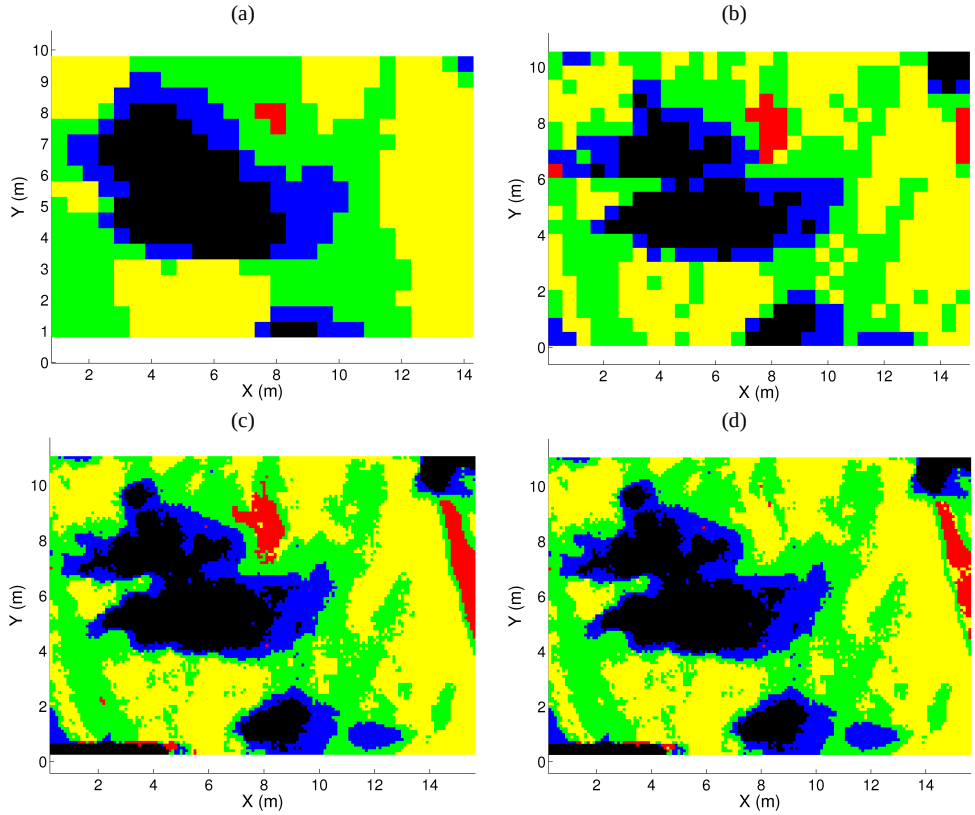

Fig. 5 Typical results from the automatic treatment of a greyscale image (procedure 3) from 8th June 2006 (Fig. 2a) into the five different classes (same legend as for Fig. 4) for different values of l_f and Δx: (a) l_f = 40 pxl and Δx = 10 pxl ; (b)) l_f = 10 pxl and Δx = 10 pxl ; (c)) l_f = 10 pxl and Δx = 2 pxl ; (d)) l_f = 10 pxl and Δx = 2 pxl with the delimitation between fines deposits and coarse sediments switched from *ph* = 205 to 190.

The surface (estimated from procedure 2) represents approximately one third of the total surface of the gravel bar. However, the common surface is only of 760 m^2 (10% of the total surface of the gravel bar). It corresponds to stable deposits, i.e. bar tail, downstream part of the secondary channel, or in the wake of stable obstacle (vegetation, large trunks, blocks). In the edge of the gravel bar, one can observe deposits before and after the event but the location between of the deposits varies between both states.

The same pictures were processed using procedure 3 (Fig. 7 and Tab. 2). The location of the deposits corresponds roughly to what was found using procedure 1. The use of l_f = 10 pxl appears more accurate to estimate surfaces but the use of l_f = 40 pxl yields more readable pictures for the whole gravel bar. If l_f = 10 pxl is used, the estimated surfaces of deposits are similar to those obtained from the manual methodology (450 m^2 compared to 810 m^2 before the flushing event and 1,880 m^2 compared to 1,590 m^2 after the flushing event. Even if uncertainties are relatively large, one can say

Author-produced version of the article published in International Journal of Sediment Research (2013), Vol. 28, Iss. 2, 220–233
The original publication is available at http://www.sciencedirect.com/ doi:10.1016/S1001-6279(13)60033-5

that procedure 3 reproduces results from procedure 1. It is also possible to give an estimate of the total surface covered by fine deposits assuming typical surface coverage for classes (b1) (b2), and (d). We obtained a surface equal to 3,200 m^2 before the flushing event and equal to 3,400 m^2 before the flushing event using l_f = 10 pxl. Even though the total estimated surface is 70% larger than the one estimated from procedure 2, a similar conclusion can be made: the total coverage of fine sediment deposits is stable after the 2006 flushing event.

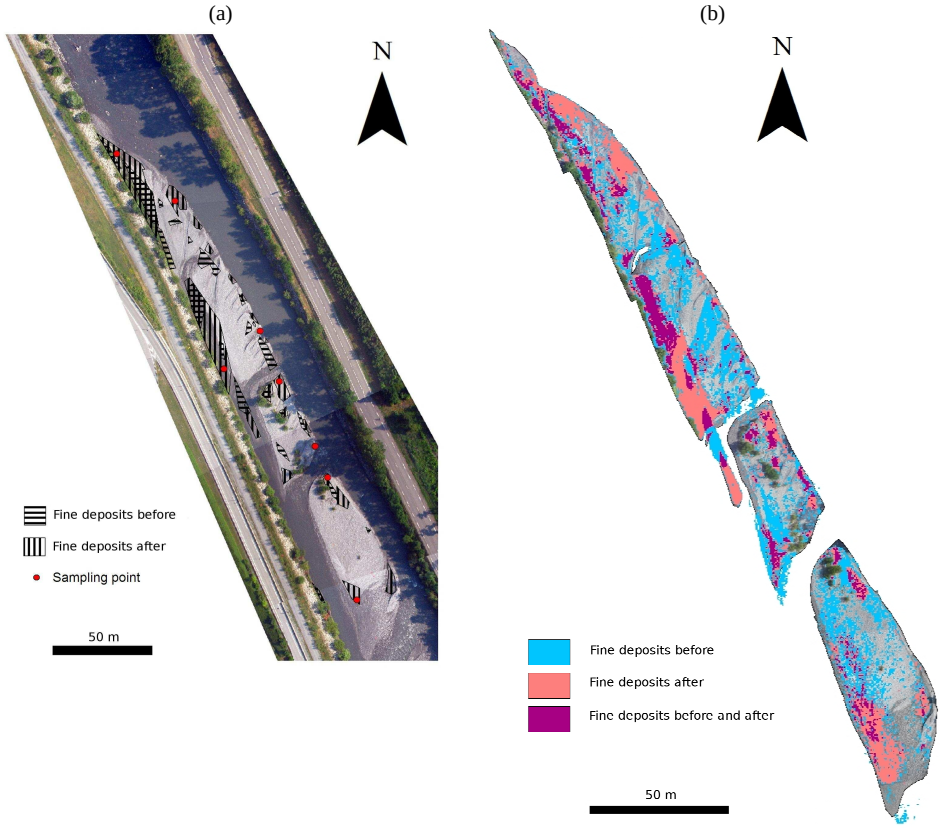

Fig. 6 Fine sediment deposits before and after the 2006 flushing event using (a) patch contours manually digitized using ArcMap tools (procedure 1) or (b) the methodology described in section 2.2.2. (procedure 2).

Table 2 Estimated surfaces in m^2 for the different classes before and after the 2006 flushing event (procedure 3)

Description	6th June 2006		5th July 2006	
	l_f = 40 pxl	l_f = 10 pxl	l_f = 40 pxl	l_f = 10 pxl
Fine deposits (d)	140	930	450	1,880
Mixture of fine and coarse sediments (b1)	1,810	2,250	1,470	1,560
Mixture of coarse and fine sediments (b2)	5,140	4,580	3,460	2,890
Coarse sediments (c)	160	230	2,320	2,450
Hidden surface (a)	540	820	190	285
Total estimated surface of the gravel bar	7,790	8,820	7,890	9,070

Author-produced version of the article published in International Journal of Sediment Research (2013), Vol. 28, Iss. 2, 220–233
The original publication is available at http://www.sciencedirect.com/ doi:10.1016/S1001-6279(13)60033-5

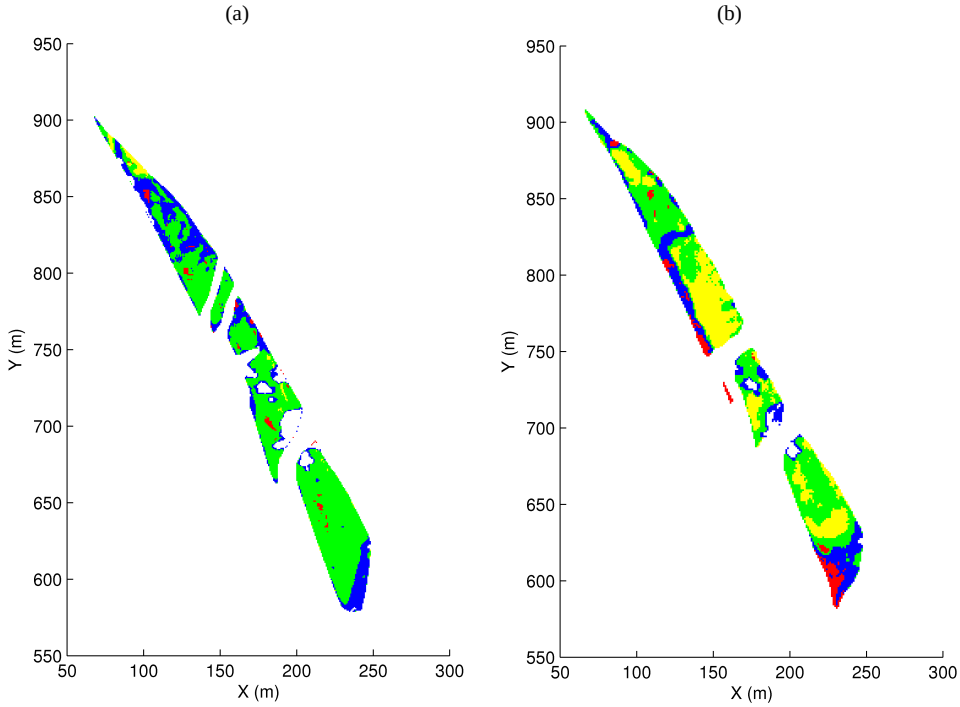

Fig. 7 Automatic treatment of the surface grain size (a) before and (b) after the 2006 flushing event using the methodology described in section 2.2.3. (procedure 3 with l_f = 40 pxl); same legend as for Fig. 4.

3.2 Results for the 2010 flushing event using procedure 3

Results obtained for the 2010 event using the automated method developed in section 2.2.3 (procedure 3) are presented in Fig. 8 and in Table 3. The main limitation of this survey should be reminded: because the pictures were taken from the side bank and because of the vegetation, part of the secondary channel could not be captured. There are also some additional difficulties due to the orthorectification of images taken with a relatively low angle and with a varying bed level. Moreover, since pictures were not taken exactly with the same position and angle for the two surveys, and since the discharge was different for both surveys, one can also observed a small difference in the total estimated surface of the gravel bar (900m^2 approximately). To treat common part between two pictures, an order of priority was affected to the classes : (a) < (b1) < (b2) < (c) < (d). One can also notice some non-physical contours of fine deposits, which correspond to limits between two pictures. This could be improved using an smoothing filter.

Although the analysis is biased in the secondary channel, very similar results to the 2006 event may be observed. The extent of large fine deposits is estimated as twice smaller before the flushing event than after the flushing event (see Table 3; one should keep in mind that procedure 3 only captures large deposits and is quite sensitive to the size of the window, l_f). On the other hand, surfaces corresponding to a mixture of fine and coarse sediment ((b1) and (b2)) are much larger before the flushing event. And the surface corresponding to clear coarse sediments significantly increased after the flushing event. An estimate of the total surface covered by fine deposits assuming typical surface coverage for classes (b1) (b2), and (d) yields the following results using l_f = 10 pxl: 3,300 m^2 before the flushing event and 4,300 m^2 after the flushing event. The total coverage of fine sediments seems to have increased by 25% after the flushing event. But again, results are very similar to the 2006 event: approximately one third of the gravel bar surface is covered by fine sediment deposits.

Author-produced version of the article published in International Journal of Sediment Research (2013), Vol. 28, Iss. 2, 220–233
The original publication is available at http://www.sciencedirect.com/ doi:10.1016/S1001-6279(13)60033-5

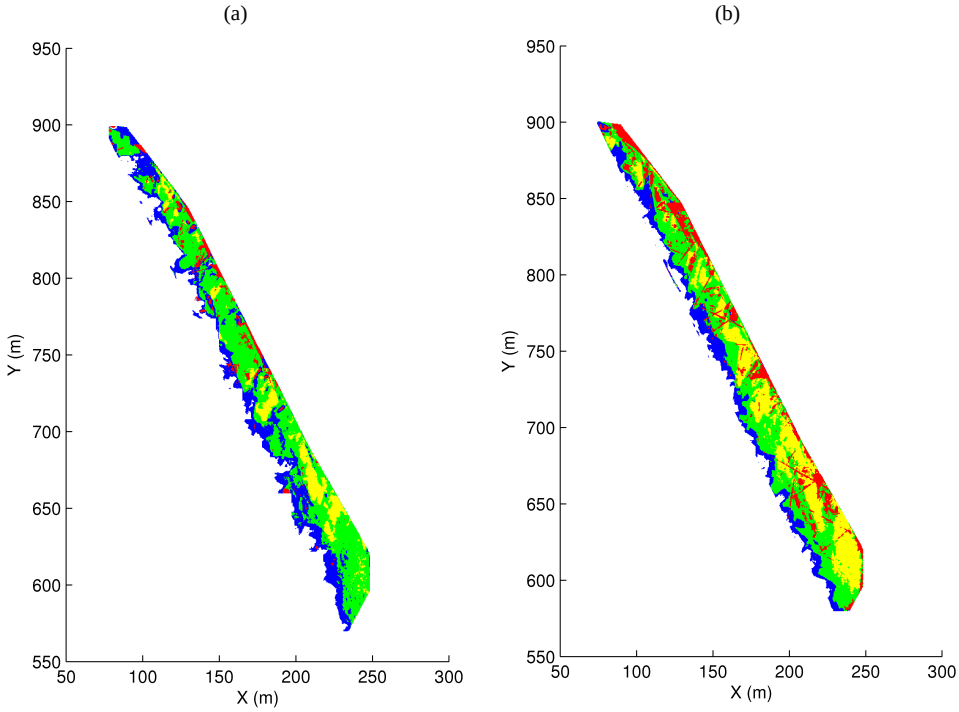

Fig. 8 Automatic treatment of the surface grain size (a) before and (b) after the 2010 flushing event using the methodology described in section 2.2.3. (procedure 3 with l_f = 40 pxl); same legend as for Fig. 4.

Table 3 Estimated surfaces in m^2 for the different classes before and after the 2010 flushing event (procedure 3).

Description	3rd June 2010		9th June 2010	
	l_f = 40 pxl	l_f = 10 pxl	l_f = 40 pxl	l_f = 10 pxl
Fine deposits (d)	500	1,450	1,780	3,050
Mixture of fine and coarse sediments (b1)	2,350	2,060	970	1,350
Mixture of coarse and fine sediments (b2)	4,310	3,200	2,670	2,570
Coarse sediments (c)	960	1,260	2,790	2,150
Hidden surface (a)	1,660	60	970	110
Total estimated surface of the gravel bar	8,300	8,040	9,180	9,230

3.3 Application of the procedure 3 on aerial pictures from LiDAR surveys

Some additional aerial photographs were available from two LiDAR surveys carried out in 9th May and 5th September 2010, respectively. Images were taken from a helicopter flying 600 m above the ground using a Hasselblad camera with a 50 mm objective. The image resolution is of 0.08 m. The automatic treatment was also applied on these images following steps in procedure 3. However, the suggested threshold values for the definition of the five classes (see Tab. 1) had to be modified to better capture the different classes. This could be explained the lower definition (0.08 m instead of 0.04 m) affecting the texture of the images and so implying a larger value for *mh* to discriminate fine sediment deposits (*mh* > 0.05). Moreover, the May 2010 pictures appeared much darker implying also a shift for the *ph* thresholds (*ph* ≤ 80 for vegetation, 80 < *ph* ≤ 140 for a fine and coarse sediment mixture, 140 < *ph* ≤ 180 for a coarse and fine sediment mixture, and *ph* ≤ 180 coarse sediments). Final results are presented in Table 4.

Author-produced version of the article published in International Journal of Sediment Research (2013), Vol. 28, Iss. 2, 220–233
The original publication is available at http://www.sciencedirect.com/ doi:10.1016/S1001-6279(13)60033-5

Table 4 Estimated surfaces in m^2 for the different classes in May and September 2010.

Description	9th May 2010		5th September 2010	
	l_f = 40 pxl	l_f = 10 pxl	l_f = 40 pxl	l_f = 10 pxl
Fine deposits (d)	300	710	300	1,650
Mixture of fine and coarse sediments (b1)	4,520	4,050	2,310	2,130
Mixture of coarse and fine sediments (b2)	6,590	5,650	8,700	7,250
Coarse sediments (c)	110	190	10	60
Hidden surface (a)	100	290	290	550
Total estimated surface of the gravel bar	11,600	11,650	11,600	11,650

In the same way as for the survey just before and after the flushing event, it appears that the detection of the fine deposits is sensitive to the size of the moving research window. Even if the quality of the picture does not allow us to conclude definitely, a similar conclusion as for the flushing event may be given: large deposits that are expected to appear just after an event seem to slowly disappear with time and to be scattered all over the gravel bar, mixed with coarser sediments. On 5th September 2010, that means three months after the last major event (200 m^3/s flood), only a few fine deposit patches are remaining. On 9th May 2010, corresponding nearly to one year after the last major event (flushing event in June 2009), even less fine deposit patches were observed. However, the differences observed between this survey and the one before the dam flushing (3rd June 2010) give an indication of the accuracy of the method depending on the quality of the pictures. An estimate of the total surface covered by fine deposits assuming typical surface coverage for classes (b1) (b2), and (d) yields the following results using l_f = 10 pxl: 4,100 m^2 in May and 4,500 m^2 in September, i.e. approximately one third of the total surface of the gravel bar.

3.4 Discussion

Observations made from both surveys (2006 and 2010) lead us to use and complete the specific typology developed by Wood and Armitage (1999), defining four main types of deposits: marginal deposits, secondary channel deposits, fine superficial laminae deposits, and obstruction and vegetation deposits. As presented previously, this typology can be detailed with a percentage of the total surface estimated for each type of deposits. This estimate is more accurate using 2006 survey since there is less bias due to image orthorectification and margin vegetation (aerial image).

- Marginal deposits: They are located at the channel margin where the flow velocities are lower than those in the main channel (see Fig. 9a). These deposits occur mainly in the nooks (marginal backwater areas). The bar tail is included in marginal deposit areas as a reduced flow velocity area with backwater patterns due to the interaction with the main channel especially during the ebb part of the flow. This type of deposit is the largest component of surface deposits. It corresponds approximately to 50% of the total surface of deposits based on the procedure 2 (after 2006 event), and 60% based on the procedure 3 (after 2010 event).
- Secondary channel deposits: They are located in the downstream part of the secondary channel where flow velocities are very reduced due to quasi-horizontal bed slope (see Fig. 9a). This type of deposit represents 35% of surface deposits based on the procedure 2 (after 2006 event), and 25% based on the procedure 3 (after 2010 event).
- Fine surficial laminae deposits: They are very thin layers of fine sediment on the surface of gravel. They can be observed at the upstream part of the bar head or near the connecting channels (see Fig. 9b). Based on procedure 2 (after 2006 event), this class only represents 10% of surface. Based on procedure 3 and assuming 30% of the class “mixture of coarse and fine sediments” corresponds to fine deposits, this type of deposits covers 20% of the total surface of deposits (after 2010 event).
- Obstruction and vegetation deposits: They are located in the lee of larger substrate or shrub (see Fig. 2d for procedure 2 and Fig. 5c for the same processed image using procedure 3). They can also be located at the stand of macrophytes. This kind of deposits is generally not easy to identify on aerial photographs as it is space-limited. This category represents 5% of surface deposits but may be the thickest type of deposits (based on the 2006 event).

For both flushing events, no significant variation of the total deposit surface before and after the event was observed and this surface was approximated to one third of the total gravel bar surface. But the form and location of these deposits vary significantly before and after the event. Before the event, there are less large homogeneous deposits and fine sediments are generally mixed with coarse sediments. After the events, fine deposits correspond mainly to large homogeneous deposits, which were formed during the ebb part of the event where water depths and velocities become small in secondary channels and nooks.

Author-produced version of the article published in International Journal of Sediment Research (2013), Vol. 28, Iss. 2, 220–233
The original publication is available at http://www.sciencedirect.com/ doi:10.1016/S1001-6279(13)60033-5

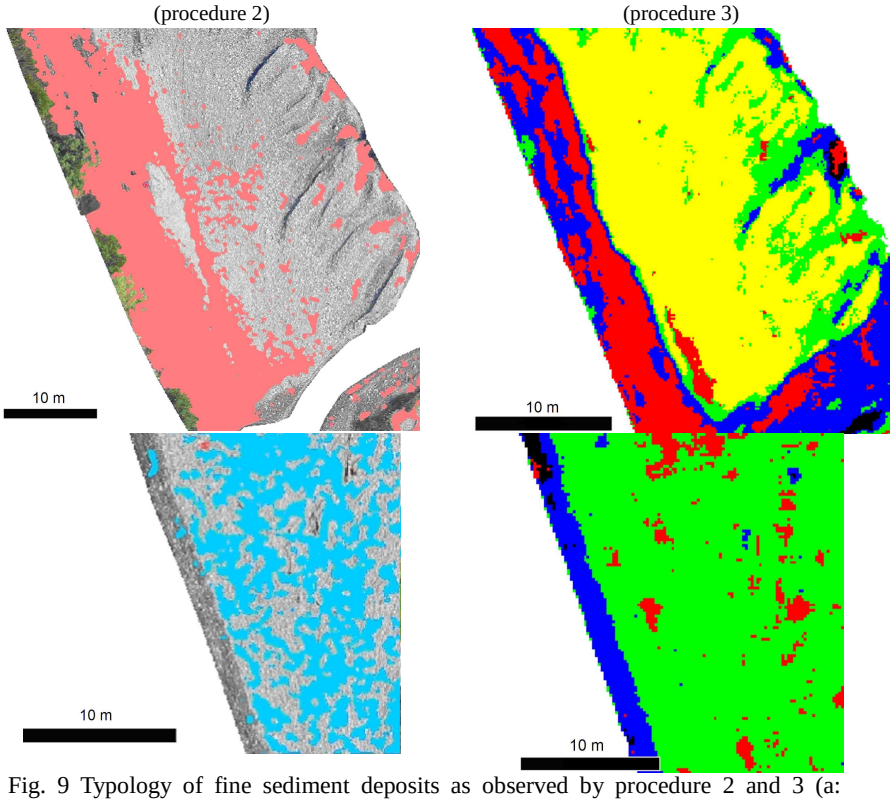

Fig. 9 Typology of fine sediment deposits as observed by procedure 2 and 3 (a: secondary channel deposits (left part of the images) and marginal deposits (right part of the images); b: fine surficial laminae deposits).

A grain size analysis showed that the median grain size of the deposits (d_{50}≈150 μm on average) is much coarser than the median grain size of the suspended sediments during the event (d_{50}≈20 μm on average) with only 10% of the fraction in common. Thus, a clear distinction should be made between wash load and suspension of fine sediments close to the bed. The total area of fine deposits in vegetation zones and in topographic depressions shows the significant part of these particular bar components to the fine sediment budget. Although a large flood in May 2008 significantly modified the morphodynamics of the gravel bar (erosion of the main channel that limits the flooding of the gravel bar), similar observations were made for both events (2006 and 2010), indicating that the duration of the bar inundation does not have a significant impact. Vegetation on the gravel bar, which was totally swept away after the may 2008 flood, does not affect as significantly as one could believe the dynamics of fine sediment deposit. Indeed, it represents less than 5% of the total deposits. It should be interesting to check if a natural flood with high sediment load affects the fine deposit dynamics similarly. Results from the LiDAR survey on 5th September 2010 do not allow us to conclude since a three month period separate this survey from the previous natural flood (200 m^3/s flood). Only a few fine sediment patches were remaining. From this study, large deposits being observed just after a flushing event seem to be scattered with time all over the gravel bar, mixed with coarser sediments. A possible hypothesis to explain this phenomena could be a dispersion due to rain and wind transport.

4 Conclusions

Three methods to estimate fine deposit surface were presented and discussed. A manual digitization and two automated procedures were achieved using aerial pictures dated 2006 whereas only the second automated procedure was achieved using pictures taken in 2010 from a high-lift truck set on the side bank of the river. The three methods yield similar results although only the automated procedure with Envi4.3 was capable to capture small deposits. This method appeared to be the most effective but it also require an imposition of threshold values, which have to be recalibrated for each set of pictures. Another drawback could also be the cost of an Envi4.3 software licence. The second automated procedure (procedure 3) based on a simple characterisation of a window histogram was validated on the 2006 event and yields very similar results as the first automated procedure (procedure

Author-produced version of the article published in International Journal of Sediment Research (2013), Vol. 28, Iss. 2, 220–233
The original publication is available at http://www.sciencedirect.com/ doi:10.1016/S1001-6279(13)60033-5

2). The interest of both automated procedures is that they can be easily applied to relatively large pictures (or a mosaic of pictures) as soon as criteria for the different classes are correctly calibrated. A manual digitalization remains influenced by the operator choice. Both automated methods need however a calibration of threshold values for each set of pictures depending on image resolution and exposures.

Automated methods can be applied not only to estimate fine sediment deposits but also to other coarser classes of sediments. If the quality/resolution of the pictures is good enough, they could be applied to estimate surface grain size of the sediments (Carbonneau et al., 2005a and b). These methods are however sensitive to photos exposure and to shadows. Nevertheless, from these automated procedures, we were able to distinguish main types of deposits as defined by Wood and Armitage (1999), and to give an estimate of their surficial extent after a flushing event.

Based on all these surveys, it appeared that the overall coverage of fine sediment deposits over the gravel bar is fairly constant and corresponds approximately to one third of the gravel bar surface. However, the location of these deposits differ significantly before and after an event. Larger (and maybe thicker) marginal and secondary channel deposits are observed after an event. There is also a remaining query about the formation of the initial state (before the flushing event): since the gravel bar is rarely submerged in winter and spring: what is the part of rain and wind transport in the redistribution of fine deposits?

One of the issues not specifically addressed by this paper is the estimate of the ratio of fine sediment infiltrated into the gravel bed. Visual observations in the field confirmed that deposit thickness may vary considerably depending on the type of deposits and revealed that the first 50 cm deep gravel-bed interstices were almost filled with fine sediments. There is a need of evaluating volumes of fine sediments over the gravel bar in order to distinguish different processes such as deposition, and resuspension as well as infiltration.

Acknowledgements

This study was supported by Irstea. Authors are grateful to people who took part in the field surveys, in particular technicians (G. Dramais, T. Fournier, M. Lagouy and F. Thollet) and UMR 5600 CNRS. The two anonymous referees are thanked for their critical comments and suggestions, which substantially improved the original manuscript.

References

Brandt, S. 1999, Sedimentological and geomorphological effects of reservoir flushing: The Cachi reservoir, Costa Rica, 1996. Geografiska Annaler A, Vol. 81, pp. 391–407.

Carbonneau, P. E., Bergeron, N. E. et Lane, S. N. 2005a, Texture-based image segmentation applied to the quantification of superficial sand in salmonid river gravels. Earth Surface Processes and Landforms, Vol. 30, pp. 121–127.

Carbonneau, P. E., Bergeron, N. E. et Lane, S. N. 2005b, Automated grain size measurements from airborne remote sensing for long profile measurements of fluvial grain sizes. Water Resources Reseach, Vol. 41, No. W11426, pp. 1-9

Carbonneau, P. E., Lane, S. N., and Bergeron, N. E. (2004), Catchment-scale mapping of surface grain size in gravel bed rivers using airborne digital imagery, Water Resources Research, Vol. 40, No. W07202, pp.1-11.

Fausch, C. D., Torgersen, C. E., Baxter, C. V. and Li, H. W. (2002), Landscapes to riverscapes: Bridging the gap between research and conservation of stream fishes, Bioscience, Vol. 52, pp. 483-498.

Folks, R. L., and Ward, W. C. (1957). Brazos River bar: A study in the significance of grain size parameters. Journal of Sedimentary Petrology, Vol. 27, No. 1, pp. 3-26.

Grams, P.E., Schmidt, J.C. (2002). Streamflow regulation and multi-level flood plain formation: channel narrowing on the aggrading Green River in the eastern Uinta Mountains, Colorado and Utah. Geomorphology, Vol. 44, pp. 337-360.

Hauet, A. 2006, Estimation de débit et mesure de vitesse en rivière par Large-Scale Particle Image Velocimetry [Discharge estimates and velocity measurements using Large-Scale Particle Image Velocimetry] PhD thesis, INP Grenoble, France (in French).

Jodeau M. 2007a, Morphodynamique d'un banc de galets en rivière aménagée lors de crues [Gravel bar morphodynamics in an engineered river during high flow events]. PhD thesis, Claude Bernard University, Lyon 1 (in French).

Jodeau M., Paquier A., Hauet, A., Le Coz, J., Thollet F., and Fournier, T. 2007b, Effect of a reservoir release on the morphology of a gravel bar: Field observations and 2Dh modeling, Proceedings of RCEM conference 2007, pp. 1029-1036.

Kondolf, G. M. and Wilcock, P. R. (1996) The flushing flow problem: Defining and evaluating objectives. Water Resources Research, Vol. 32, No. 8, pp. 2589-2599.

Konrad, C. P., Both, D. B., Burges, S. J., and Montgomery, D. R. (2002). Partial entrainment of gravel

bars during floods. Water Resources Research, Vol. 38, No. 7, pp. 1-16.

Lisle T. 1989, Sediment transport and resulting deposition in spawning gravels, North Coastal California. Water Resources Research, Vol. 25, pp. 1303–1319.

Liu, J., Minami, S., Otsuki, H., Liu, B., and Ashida, K. (2004). Environmental impacts of coordinate sediment flushing." J. Hydraul. Res., Vol. 42, No. 5, pp. 461–472.

Lyon, J. G., Lunetta, R. S. , and Williams D. C. (1992), Airborne multispectral scanner data for evaluating bottom sediment types and water depths of the St. Mary's River, Michigan, Photogramm. Eng. Remote Sens., Vol. 58, pp. 951–956.

Ma, Y., Huang, H. Q, Nanson, G. C., Li Y., and Yao, W., 2012, Channel adjustments in response to the operation of large dams: The upper reach of the lower Yellow River, Geomorphology, Vol. 147–148, pp. 35–48

Rathburn S. and Wohl E. 2003, Predicting fine sediment dynamics along a pool riffle mountain channel. Geomorphology, Vol. 55, pp. 111–124.

Rubin, J., Glimsater, C. and Jarvi, T. (2004). Characteristics and rehabilitation of the spawning habitats of the sea trout, Salmo trutta, in Gotland (Sweden). Fisheries Management and Ecology, Vol. 11, pp. 15-22.

Verdúa, J. M., Batallab, R. J., and Martínez-Casasnovas, J. A. (2005). High-resolution grain-size characterisation of gravelbars using imagery analysis and geo-statistics. Geomorphology, Vol. 72, No. 1-4, pp. 73-93.

Wang, E. and Cenderelli, D. 2000, Sediment deposition and transport patterns following a reservoir sediment release. Water Resources Research, Vol. 15, pp. 319–333.

Wohl, Y.-H., Wang, Y.-H. and Tang, L.-Q. 2008, On the formation of couplet-style stratifications. International Journal of Sediment Research, Vol. 23, pp. 85-91

Wood, P. and Armitage, P. 1997, Biological effects of fine sediment in the lotic environment. Environmental Management, Vol. 21, pp. 203–217.

Wood, P. and Armitage, P. 1999, Sediment deposition in a small lowland stream - Management implications. Regulated Rivers: Research and Management, Vol. 15, pp. 199-210.